Radiative magnetohydrodynamic nanofluid flow due to gyrotactic microorganisms with chemical reaction and non-linear thermal radiation

Muhammad Ramzan, Jae Dong Chung, Naeem Ullah

PII: S0020-7403(17)30843-3
DOI: 10.1016/j.ijmecsci.2017.06.009
Reference: MS 3737

To appear in: *International Journal of Mechanical Sciences*

Received date: 2 April 2017
Revised date: 17 May 2017
Accepted date: 7 June 2017

Please cite this article as: Muhammad Ramzan, Jae Dong Chung, Naeem Ullah, Radiative magnetohydrodynamic nanofluid flow due to gyrotactic microorganisms with chemical reaction and non-linear thermal radiation, *International Journal of Mechanical Sciences* (2017), doi: 10.1016/j.ijmecsci.2017.06.009

Highlights

- Nanofluid with Motile gyrotactic microorganisms is discussed in this exploration.
- The study is explored under the response of non-linear thermal radiation.
- Convective heat and mass boundary conditions are also used.
- Runge-Kutta fourth-fifth order Fehlberg technique is used to solve the problem.
- To validate our results, a comparison to previous study is also added.

GraphicalAbstract

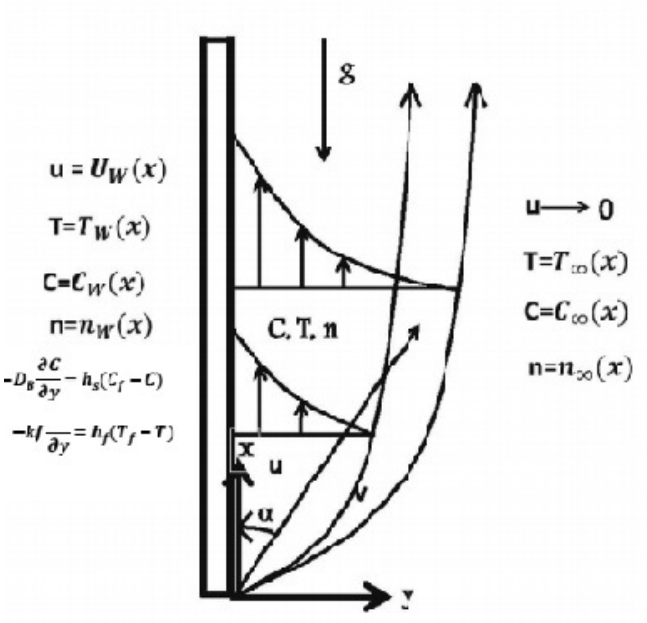

Radiative magnetohydrodynamic nanofluid flow due to gyrotactic microorganisms with chemical reaction and non-linear thermal radiation

Muhammad Ramzan [*a, b], Jae Dong Chung[b], and Naeem Ullah[c]

[a] *Department of Computer Science, Bahria University Islamabad Campus, Islamabad, Pakistan.*
[b] *Department of Mechanical Engineering, Sejong University, Seoul143-747, Korea.*
[c] *Department of Mathematics, Quaid-i-Azam University, Islamabad, Pakistan.*

Abstract

This study investigates the heat and mass transfer of nanofluid with motile gyrotactic microorganisms. The study is explored under the response of non-linear thermal radiation, viscous dissipation and Joule heating effects. The slip and convective convective boundary conditions are also taken into account. The coupled partial differential equations are reduced to nonlinear ordinary differential equations using appropriate transformations. The differential equations are solved numerically by using Maple dsolve command with option numeric which utilize Runge-Kutta fourth-fifth order Fehlberg technique. A comparison to the previous study is also included to validate the present results. The evaluations are carried out for sundry parameters on flow, heat transfer and motile density of microorganisms. It is observed that the motile density of microorganisms shows a decreasing behavior for growing values of bioconvection lewis number and Peclet number.

Keywords: Bioconvection; gyrotactic microorganisms; non-linear thermal radiation; Joule heating; viscous dissipation; slip and convective boundary conditions.

*Corresponding author e-mail address: mramzan@bahria.edu.pk

1 Introduction

Electrically conducting fluids with magnetic properties lead to the term magnetohydrodynamic (MHD). The study of MHD has gained significant attention of researchers and scientists because of its varied applications in engineering and biological sciences. It is used to heat, pump, stir and levitate liquid metals. The static magnetic field is applied for the laminarization of contactless damping turbulent flow in the formation of semiconductor crystals or the continuous casting of steel. In addition, since the rate of cooling is crucial for the quality of a product, thus magnetohydrodynamic is used in several manufacturing methods to manage the rate of cooling. Recently, MHD was conjointly found helpful in several disease diagnostic processes. Thus, flows under the effect of MHD receive the considerable attention of many researchers. Among well known studies on this subject, Mustafa et al. [1] considered the effect of MHD and bouncy forces on the flow of nanofluid over a vertical sheet in the presence of chemical reaction and activation energy. Ramzan et al. [2] discussed the flow of Jeffrey nanofluid affected by MHD along a stretching vertical plate with joule heating and thermal radiation. Likewise Hussain et al. [3] considered the MHD flow over a stretching cylinder in the presence of joule heating and viscous dissipation effects. In another study, Khan et al. [4] investigated magnetohydrodynamic stagnation flow of nanofluid impinging obliquely on the horizontal plate.

Efficient thermal conductivity requirements are continuously increasing due to faster speed (in the multi-GHz range) and smaller size for microelectronic devices. Cooling of such gadgets has become one of the top technical challenge faced by high-tech industries such as microelectronics and automotive. These industries are in dire need to revise and adopt new technologies that could provide effective and efficient heat transfer amenity. Simple base fluids like water and ethylene glycol do not possess the required thermal conductivity properties. However, the mixture of small sized metal particles in these base fluids named as "Nanofluids" are more effective in heat transfer rate. Nanofluids are the colloidal suspensions of nanomaterials which are prepared by dispersing nanometer-sized materials, (i.e., nanoparticles, nanofibers, nanotubes, nanowires and nanorods) along with the base fluids. Water, oil, and ethylene glycol are commonly used base fluids. Choi et al. [5] introduced the concept of nanofluids in order to generate fluids with higher thermal conductivity and heat transfer rate. Nanofluids have extraordinary characteristics that make them potentially useful. Due to the wide range of applications they after received sig-

nificant attention. Nanofluids are used as cooling agent in electronic equipment, vehicles, heavy-duty engine and in industries to enhance the efficiency, save energy and reduce emissions. Nanofluids have also some biomedical applications, like in antibacterial and drug delivery. Consequently nanofluids represent an area of interest for many researchers and scientists due to a wide range applications. Some of the recent explorations may include study by Sheikholeslami and Ganji [6] who investigated numerically the flow of nanofluid containing copper nanoparticles in the presence of uniform magnetic field effect. Rashidi et al. [7] found an analytic and numerical solution of viscous water based nanofluid with second order slip condition using fourth order RK method together with shooting iteration method. Mehmood et al. [8] examined oblique Jeffery nanofluid flow near a stagnation point using Optimal Homotopy analysis method. Likewise author's in [9] explored analytical solution of Oldroyd-B nanofluid flow with heat generation/absorption past a stretched surface Some admissible investigations by the researchers about nanofluids can be found in [10–17].

Bioconvection is the spontaneous pattern development in the swimming microorganisms. Like natural convection, bioconvection occurs due to the unstable stratification, i.e., it is caused by the up swimming of microorganisms like algae which form a concentrated layer on the upper surface of the fluid. Microorganisms are slightly denser than water [18, 19]. Generally, the microorganisms swim upwards and the reason for up swimming is different for different species [20]. The stimulator which tends the self-propelled microorganisms to swim in particular directions include oxygen concentration gradient. The microorganisms transport, oxygen and cells, from upper region of fluid to the lower region. The response of microorganisms to stimulators is known as taxes. Amongst these movements, some are gravitaxis, chemotaxis, gyrotaxis and phototaxis. The movement of microorganisms is in the opposite direction to gravity, up a chemical gradient and towards or away from light. Gyrotaxis is controlled by the torque due to gravity and the viscous shear forces on bottom-heavy cell (some algae and bacteria), so in gyrotaxis, the cells tend toward downwelling fluid. Microorganisms that are involved in bioconversion phenomenon are the bottom-heavy algae (Chlamydomonas nivalis) and common soil bacterium (B. subtilis). Comprehensive discussions on the response of microorganisms can be found in [21–26]. Unlike motile microorganisms, the nanofluids are not self-propelled and their motion is characterized by Brownian motion and thermophoresis. Adding microorganisms to the suspension of nanofluid improve its stability to enhance mass transfer (in bio-microsystem)

and prevent nanoparticles from forming a dense cluster [27–29]. Kuzentsov [30] scrutinized the nanofluid bioconvection which is characterized by nanoparticles, oxytactic microorganisms, and temperature variations. Noreen and Khan [31] explored the bioconvection in the presence of gyrotactic microorganisms and nanoparticles along a stretching cylinder. Tham et al. [32] described the mixed convection flow in the presence of gyrotactic microorganisms in a porous medium. Aziz et al. [33] disclosed nanofluid free convection flow in a porous medium containing gyrotactic microorganisms. Khan and Makinde [34] worked out the MHD flow of water based nanofluid in the presence of gyrotactic microorganisms over a stretching sheet. Mutuku and Makinde [35] investigated MHD bioconvection nanofluid flow due to gyrotactic microorganisms along a permeable vertical sheet. Mehrayan et al. [36] studied the effect of a non-uniform magnetic field on a nanofluid that contains gyrotactic microorganisms along a nonlinear stretching vertical sheet. Some more investigations highlighting nanofluid bioconvection may be found at [37–44].

On analyzing the literature presented above, it is revealed that magnetohydrodynamic effect on bioconvection nanofluid flow in the presence of gyrotactic microorganisms under the influence of non-linear thermal radiation, chemical reaction, slip and convective boundary conditions has not been studied yet. Thus, our prime focus in this study is on five aspects. Firstly, to examine effects of magnetohydrodynamics through heat, mass and motile density flow. Secondly, to address non-linear thermal radiation. Thirdly, to analyze chemical reaction. Fourthly, to analyze the flow in the presence of Brownian motion and thermophoresis. Fifth to perform whole analysis in the presence of slip, heat and mass convective boundary conditions. The problem is solved numerically by dsolve/numeric (Runge-Kutta Fehlberg fourth and fifth order) built-in Maple 18 [45]. The results are discussed in graphical and tabular form. A comparison between present and previous investigation is also carried out prudently.

2 Problem Formulation

Consider the steady boundary layer bioconvection flow of nanofluid past a vertically stretched plate. The nanofluid contains motile gyrotactic microorganisms. The flow behavior is examined under the influence of inclined magnetic field, non-linear thermal radiation, Joule heating, viscous dissipation and convective boundary conditions. The diagram of flow problem is given in Fig. 1. It is assumed that the plate is heated from left by convection

from fluid of temperature T_f ($T_f > T_\infty$) with heat transfer coefficient h_f, similarly the concentration in the left of the plate C_f is greater than wall concentration C_w and ambient concentration C_∞ with mass transfer coefficient hs. It is further assumed that nanoparticles have no impact on movement of microorganisms. Under these assumptions the flow problem can be formulated as

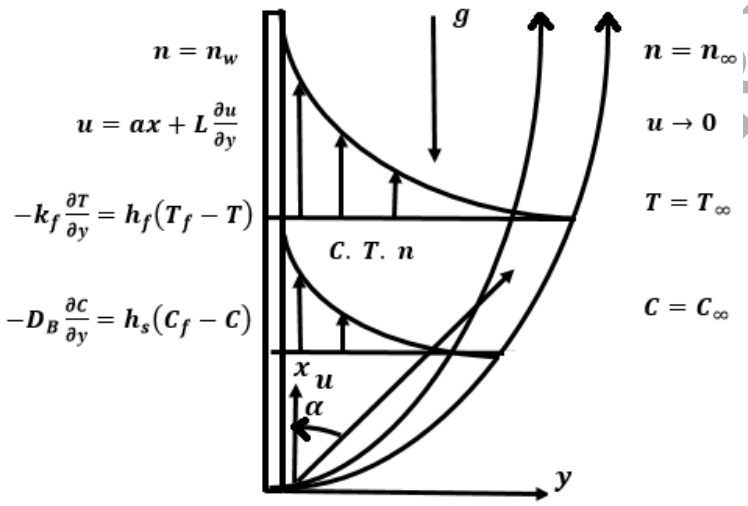

Figure 1: Flow diagram.

$$\frac{\partial u}{\partial x}+\frac{\partial v}{\partial y}=0, \tag{1}$$

$$u\frac{\partial u}{\partial x}+v\frac{\partial u}{\partial y}=\frac{\mu}{\rho_f}\left(\frac{\partial^2 u}{\partial y^2}\right)+\frac{\sigma}{\rho_f}B_0^2 sin^2\alpha u+\frac{1}{\rho_f}\left(1-C_\infty\right)\rho_f\frac{1}{\rho_f}g\beta\left(T-T_\infty\right)$$
$$-\frac{1}{\rho_f}\left(\rho_p-\rho_f\right)g\left(C-C_\infty\right)-\frac{1}{\rho_f}\left(\rho_m-\rho_f\right)g\left(n-n_\infty\right), \tag{2}$$

$$u\frac{\partial T}{\partial x}+v\frac{\partial T}{\partial y}=\frac{k}{(\rho c_p)_f}\frac{\partial^2 T}{\partial y^2}-\frac{1}{(\rho c_p)_f}\frac{\partial q_r}{\partial y}+\frac{(\rho c_p)_p}{(\rho c_p)_f}\left[D_B\frac{\partial C}{\partial y}\frac{\partial T}{\partial y}+\frac{D_T}{T_\infty}\left(\frac{\partial T}{\partial y}\right)^2\right]$$
$$+\frac{\mu}{(\rho c_p)_p}\left(\frac{\partial u}{\partial y}\right)^2+\frac{1}{(\rho c_p)_p}\sigma\beta_0^2 sin^2\alpha u^2, \tag{3}$$

$$u\frac{\partial C}{\partial x}+v\frac{\partial C}{\partial y}=D_B\frac{\partial^2 C}{\partial y^2}+\frac{D_T}{T_\infty}\frac{\partial^2 T}{\partial y^2}-k_r(C-C_\infty), \tag{4}$$

$$u\frac{\partial n}{\partial x}+v\frac{\partial n}{\partial y}+\frac{bW_c}{C_f-C_\infty}\frac{\partial}{\partial y}\left(n\frac{\partial C}{\partial y}\right)=D_m\frac{\partial^2 n}{\partial y^2}. \tag{5}$$

Using Rosseland approximation [46] of thermal radiation we get the following expression

$$q_r = -\frac{4\sigma^*}{3k^*}\frac{\partial T^4}{\partial y} = -\frac{16\sigma^*}{3k^*}T^3\frac{\partial T}{\partial y},$$

here σ^* denote Stefan Boltzmann constant and k^* is mean absorbtion coefficient. Evaluating q_r in energy equation, we obtain the following form

$$u\frac{\partial T}{\partial x} + v\frac{\partial T}{\partial y} = \frac{\partial}{\partial y}\left[\left(\alpha + \frac{16\sigma^* T^3}{3k^*(\rho c_p)_f}\right)\frac{\partial T}{\partial y}\right] + \frac{(\rho c_p)_p}{(\rho c_p)_f}\left[D_B\frac{\partial C}{\partial y}\frac{\partial T}{\partial y} + \frac{D_T}{T_\infty}\left(\frac{\partial T}{\partial y}\right)^2\right]$$
$$+ \frac{\mu}{(\rho c_p)_p}\left(\frac{\partial u}{\partial y}\right)^2 + \frac{1}{(\rho c_p)_p}\sigma\beta_0^2 sin^2\alpha u^2, \tag{6}$$

where u, v are x and y-component of velocity, B_0, α are the strength and inclination angle of magnetic field. T, q_r, C, n, μ, σ, β, γ, ρ_f, ρ_m, ρ_p, $(\rho c_p)_f$, $(\rho c_p)_p$, D_B, D_T, D_m, b, W_c and k_r, are the temperature, radiation heat flux, concentration of nanoparticles, concentration of microorganisms, viscosity of fluid suspension of nanoparticle and microorganism, electrical conductivity, volumetric thermal expansion coefficient, volume of microorganism, density of the fluid, density of microorganism, density of nanoparticle, heat capacity of fluid, heat capacity nanoparticles, Brownian diffusion coefficient, thermophoretic diffusion coefficient, diffusivity of microorganisms, chemotaxis constant, maximum speed of swimming cell and rate (constant) of chemical reaction respectively.The ambient values of temperature and concentration are indicated by T_∞ and C_∞.

The appropriate boundary conditions are follow as

$$u = ax + L\frac{\partial u}{\partial y}, v = 0, -k\frac{\partial T}{\partial y} = h_f(T_f - T), -D_B\frac{\partial C}{\partial y} = h_s(C_f - C), n = n_w : y = 0,$$
$$u \to 0,\ T \to T_\infty,\ C \to C_\infty,\ n \to n_w : y \to \infty, \tag{7}$$

where L, n_w, h_f and h_s are the slip coefficient, concentration of motile microorganisms at wall, heat and mass transfer coefficients respectively.

We introduce the following transformations to convert Equations (2 - 7) into nondimensional form:

$$\eta = \sqrt{\frac{c}{\nu}}y,\ \psi = \sqrt{a\nu_f}xf(\eta),\ \phi(\eta) = \frac{C - C_\infty}{C_f - C_\infty},\ \theta(\eta) = \frac{T - T_\infty}{T_f - T_\infty},\ \xi(\eta) = \frac{n - n_\infty}{n_w - n_\infty}. \tag{8}$$

After using the similarity transformations (8), Eq. (1) is identically satisfied however, Eqs. (2, 4, 5, 6, 7) take the form

$$f''' + ff'' - f'^2 - Hasin^2\alpha f' + \lambda(\theta - Nr\phi - Rb\xi) = 0, \tag{9}$$

$$\left[\left(1 + Rd\big(1 + (Tr-1)\theta\big)^3\right)\theta'\right]' + \Pr(f\theta' + Nb\theta'\phi' + Nt\theta'^2) + \Pr Ec\left(f''^2 + Hasin^2\alpha f'^2\right) = 0, \tag{10}$$

$$\phi'' + \left(\frac{Nt}{Nb}\right)\theta'' + Lef\phi' - A\phi = 0, \tag{11}$$

$$\xi'' + Lb\xi' - Pe\left[\xi'\phi' + (\xi + \Omega)\right] = 0, \tag{12}$$

$$\begin{aligned} &f(0) = 0, \quad f'(0) = 1 + \delta f''(0), \quad \theta'(0) = -Bi(1 - \theta(0)), \\ &\phi'(0) = -Nd(1 - \phi(0)), \quad \xi(0) = 1, \\ &f'(\eta) \to 0, \quad \theta(\eta) \to 0, \quad \phi(\eta) \to 0, \xi(\eta) \to 0 : \eta \to \infty, \end{aligned} \tag{13}$$

where

$$\begin{aligned} &Ha = \sqrt{\frac{\sigma B_0^2}{a\rho_f}}, \quad \lambda = \frac{Gr}{Re_x^2}, \quad Gr = \frac{g\beta(1 - C_\infty)\Delta T x^3}{\nu_f^2}, \quad Re_x = \frac{ax^2}{\nu_f}, \\ &Nr = \frac{(\rho_p - \rho_f)\Delta C}{\rho_f\beta(1 - C_\infty)\Delta T}, \quad Rb = \frac{(\rho_m - \rho_f)g\gamma\Delta n}{\rho_f\beta(1 - C_\infty)\Delta T}, \quad Rd = \frac{16\sigma^* T_\infty^3}{3kk^*}, \\ &Tr = \frac{T_f}{T_\infty}, \quad \Pr = \frac{\nu_f}{\alpha}, \quad Le = \frac{\alpha}{D_B}, \quad Nb = \frac{\tau D_B}{\nu_f}\Delta C, \ Nt = \frac{D_T}{T_\infty}\frac{\tau}{\nu_f}\Delta T, \\ &Lb = \frac{\alpha}{D_m}, \quad Pe = \frac{bW_c}{D_m}, \quad \Omega = \frac{n_\infty}{n_w - n_\infty}, \delta = L\sqrt{\frac{a}{\nu_f}}, \quad Bi = \frac{h_f}{k}\sqrt{\frac{\nu_f}{a}}, \\ &Nd = \frac{h_s}{D_B}\sqrt{\frac{\nu_f}{a}}, \ Ec = \frac{a^2x^2}{c_p\Delta T}. \end{aligned} \tag{14}$$

$Ha, \lambda, Gr, Re_x, Nr, Rb, Rd, Tr, \Pr, Le, Nb, Nt, Lb, Pe, \Omega, \delta, Bi, Nd$ and Ec are the Hartman number, mixed convection parameter, Grashof number, local Reynolds number, buoyancy ration parameter, bioconvection Rayleigh number, radiation parameter, temperature ratio parameter, Prandtl number, Lewis number, Brownian motion parameter, thermophoresis parameter, bioconvection Lewis number, bioconvection Peclet number, bioconvection concentration difference parameter, slip (momentum slip) parameter, Biot number, convection diffusion parameter and Eckert number (viscous dissipation parmaeter) respectively.

The skin-friction coefficient (C_f), the local Nusselt number (Nu_x), the Sherwood number (Sh_x) and the local density number (Nn_x) of motile microorganisms as

$$C_f = \frac{\tau_w}{\rho u_w^2(x)}, \quad Nu_x = \frac{xq_w}{k(T_f - T_\infty)}, \quad Sh_x = \frac{xq_m}{D_B(C_f - C_\infty)},$$
$$Nn_x = \frac{xq_n}{D_m(n_w - n_\infty)},$$
$$\tau_w = -\mu \left(\frac{\partial u}{\partial y}\right)_{y=0}, \quad q_w = -k \left(\frac{\partial T}{\partial y}\right)_{y=0} + (q_r)_w,$$
$$q_m = -D_B \left(\frac{\partial C}{\partial y}\right)_{y=0}, \quad q_n = -D_m \left(\frac{\partial n}{\partial y}\right)_{y=0}.$$

Using (8) the above expressions in non-dimensional form are given by

$$C_f Re_x^{1/2} = -f''(0), \quad Nu_x Re_x^{-1/2} = -\Big[1 + Rd\big\{1 + (Tr-1)\theta(0)\big\}^3\Big]\theta'(0),$$
$$Sh_x Re_x^{-1/2} = -\phi'(0), \qquad Nn_x Re_x^{-1/2} = -\xi'(0). \tag{15}$$

3 Numerical procedure

The system of non-linear ordinary differential equation (9 - 12) with boundary conditions (13) has been solved numerically utilizing Maple dsolve command with option numeric. This software automatically detected fourth and fifth order Runge-Kutta-Fehlberg method to solve the two-point boundary value problem. The RKF45 uses both fourth and fifth order Runge-Kutta scheme. The details of algorithm is given below

$$\begin{aligned}
K_0 &= f(x_i, \ y_i)h, \\
K_1 &= f\left(x_i + \frac{1}{4}h, \ y_i + \frac{1}{4}K_0\right)h, \\
K_2 &= f\left(x_i + \frac{3}{8}h, \ y_i + \frac{3}{32}K_0 + \frac{9}{32}K_1\right)h, \\
K_3 &= f\left(x_i + \frac{12}{13}h, \ y_i + \frac{1932}{2197}K_0 - \frac{7200}{2197}K_1 + \frac{7296}{2197}K_2\right)h, \\
K_4 &= f\left(x_i + h, \ y_i + \frac{439}{216}K_0 - 8K_1 + \frac{3680}{513}K_2 - \frac{845}{4104}K_3\right)h, \\
K_5 &= f\left(x_i + \frac{1}{2}h, \ y_i - \frac{8}{27}K_0 + 2K_1 - \frac{3544}{2565}K_2 + \frac{1859}{4104}K_3 - \frac{11}{40}K_4\right)h,
\end{aligned} \tag{16}$$

$$
\begin{aligned}
y_{i+1} &= y_i + \frac{25}{216}K_0 + \frac{1408}{2565}K_2 + \frac{2197}{4104}K_3 - \frac{1}{5}K_4, \\
z_{i+1} &= z_i + \frac{16}{135}K_0 + \frac{6656}{12825}K_2 + \frac{28561}{56430}K_3 - \frac{9}{5}K_4 + \frac{2}{55}K_5,
\end{aligned} \tag{17}
$$

where y and z are the fourth and fifth order Runge-Kutta technique. The step size can be determine as

$$h_{\text{new}} = h_{\text{old}}\left(\frac{\epsilon h_{\text{old}}}{2|z_{i+1}-y_{i+1}|}\right)^{\frac{1}{4}}$$

we have chosen $\eta_{\max} = \eta_\infty = 7$ in order to approach the asymptotic values given by the boundary conditions (13).

4 Discussion

This section depicts the impact of numerous non-dimensionalized parameters on the velocity, temperature, concentration and motile density distributions.

Figures 2 to 6 are plotted against the similarity variable η for the impact of sundry parameters on velocity profile. The graphs are plotted both in the presence and absence of slip effect. From these figures, it can be deduced that the velocity field has higher values for mixed convection parameter λ. As improving λ results in an enhancement in bouncy force which leads to turbulent boundary layer as evident in figure 2. Figure 3 depicts the decreasing behavior of velocity profile caused by increasing Ha, this is due to the development of Lorentz forces which involves the resistance to the fluid motion. Similarly increment in the angle of inclination boosts magnetic field which in turns reduce velocity, see figure 4. Decrease in velocity profile for increasing values of bioconvection Rayleigh number Rb is protrayed in figure 5. Escalating values of Rb opposes the upward motion of nanofluid. The fluid motion is also affected by higher values of bouncy ratio parameter Nr. As enhancement in opposite bouncy caused by ambient nanoparticle volume fraction results in a decrease in velocity profile This effect is shown in figure 6. Figures 7 to 9 indicate the rise in temperature caused by change in radiation parameter Rd, temperature ratio parameter Tr and Biot number Bi. The increase in Rd results in an enhancement in temperature. With an increase in Rd more heat transfer to the fluid causes thickening of the thermal boundary layer and temperature improvement. This effect is depicted in figure 7. Figure 8 shows the temperature gain for the rising values of temperature ratio

parameter Tr. As an increase in Tr correspond to greater wall temperature which enhances the temperature of the fluid. The effect of Biot number Bi (convection conduction parameter) on temperature can be observed in figure 9. Since Bi is associated with heat transfer at the surface. The increase in Bi causes improvement in thermal boundary layer which yields increase in temperature. The variation in concentration with respect to η for various parameters is depicted in figures 10 - 14. Figure 10 reveals the impact of viscous dissipation Ec on temperature profile. Since in viscous fluid motion, the kinetic energy of the fluid is transformed into internal energy of the fluid which results in an increase of fluid temperature. From figure 10, it is noted that the thermal boundary layer thickness and temperature are the increasing function of Ec. Figure 11 shows the effect of thermophoresis parameter Nt and Brownian motion parameter Nb on concentration distribution. An opposite behavior on concentration field is observed for Nb and Nt, i.e., the mass transfer decrease for increasing Nb and enhance for rising values of Nt. The impact of mixed convection parameter λ and Lewis number Le on concentration distribution is drawn in figure 12. It is seen that concentration profile decreases with the increase in values of λ and Le As an increase in Le is proportional to thinner concentration boundary layer and weaker mass diffusivity. Also it is seen that the concentration field decline as the λ increases. The influence of convection-diffusion parameter Nd on concentration distribution is presented in figure 13, a strong increase in the concentration profile is achieved with increasing Nd values. The highlights of the impact of chemical reaction parameter A on concentration field are considered in figures 14 and 15. It is reported that for constructive (or generation) and destructive (or consumption) chemical reaction the mass transfer displays increasing and decreasing behavior. The effect of Eckert number Ec on concentration profile is sketched in figure 16. It is observed that by increasing viscous dissipation effect the concentration distribution show decreasing tendency. Figure 17 indicates the effect of microorganism concentration difference parameter Ω on motile density of microorganisms. It is shown in the figure that the both the boundary layer thickness of microorganisms and density decrease for increasing values of Ω. The variations in density of motile microorganisms caused by the influence of bioconvection Peclet number Pe and Lewis number Lb is presented in figure 18. The density of microorganisms shows decreasing response to the increasing value of Pe and Le. The reason is that the growing values of Pe and Le causes a decrease in microorganisms diffusion that eventually results in a decrease in density of microorganisms. The impact of different embedding parameters on Skin-friction coefficient,

local Nusselt number, Sherwood number and motile density are calculated numerically and also presented in tables 1 to 4. From table 1, it is observed that the skin-friction coefficient decreases for increasing values of slip parameter δ, while it is an increasing function of Ha, α, Rb, and Nr. Table 2 depicts numerical values of heat transfer rate against different parameters. From the table, it is seen that heat transfer rate is affected by Brownian motion parameter Nb, thermophoresis parameter Nt and viscous dissipation parameter Ec (Eckert number) and shows diminishing tendency for rising values of these parameters, whereas it shows incremented behavior for increasing values Rd, Pr and Bi. The mass transfer rate is affected by slip parameter δ, while it is an increasing function of all other parameters as displayed in table 3. Table 4 portrays variation in motile density number versus different parameters. It is clear from the table that density number decreases for increasing values of Eckert number and gain for all other arising parameters. Comparison with Shehzad et al. [47] is given in table 5 for skin-friction coefficient, while for Nusselt number and Sherwood number with Makinde and Aziz [48] is given in table 6. A good agreement with all calculated values is observed.

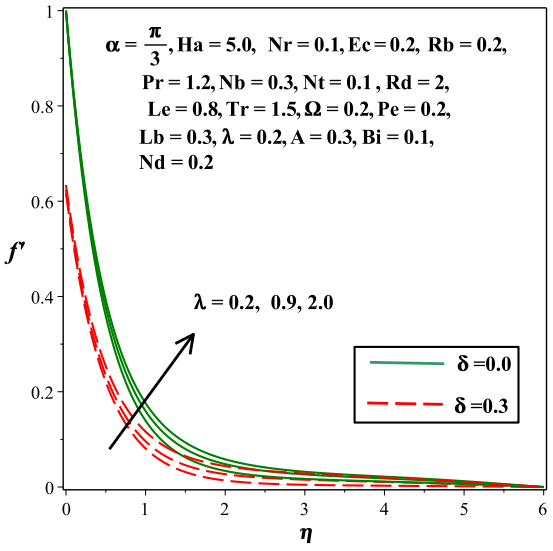

Figure 2: Impact of λ on velocity profile.

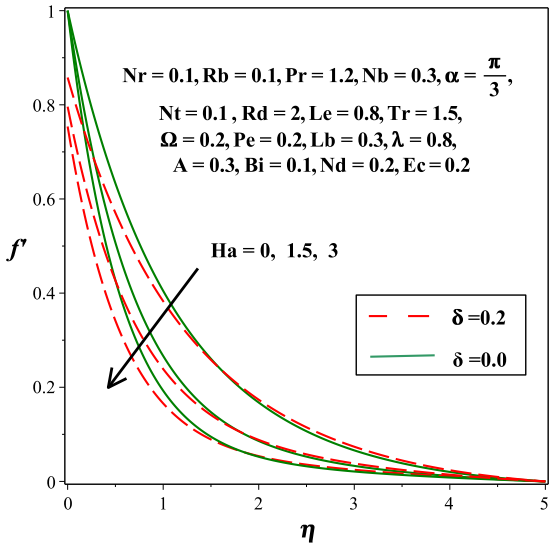

Figure 3: Impact of Ha on velocity profile.

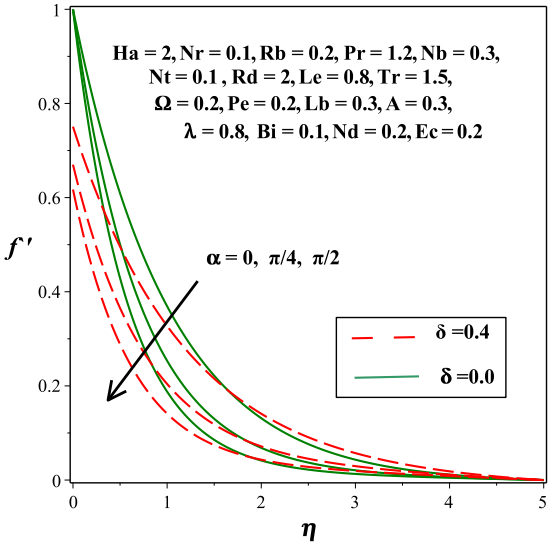

Figure 4: Impact of α on velocity profile.

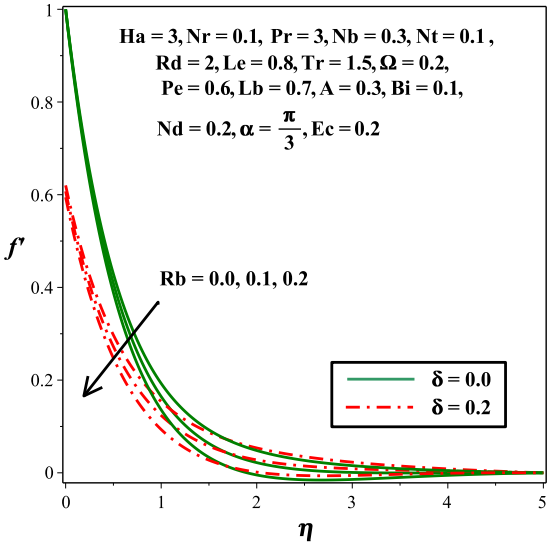

Figure 5: Impact of Rb on velocity profile.

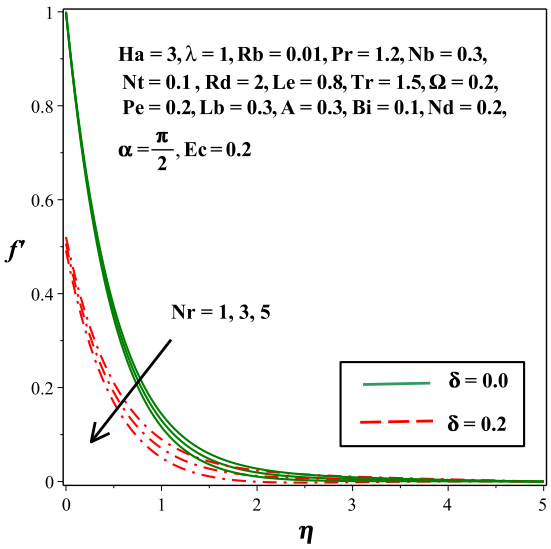

Figure 6: Impact of Nr on velocity profile.

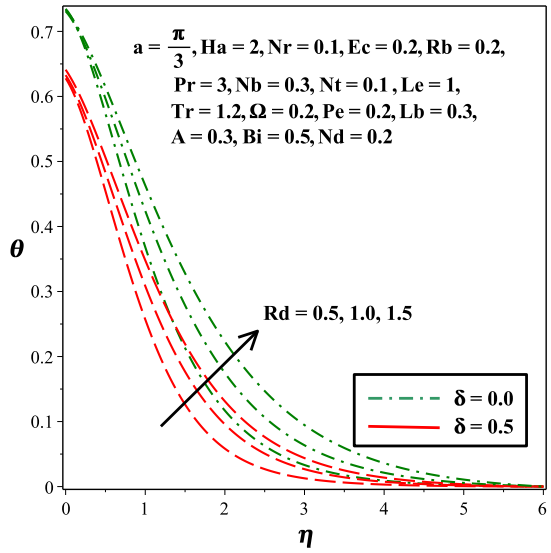

Figure 7: Effect of Rd on temperature field.

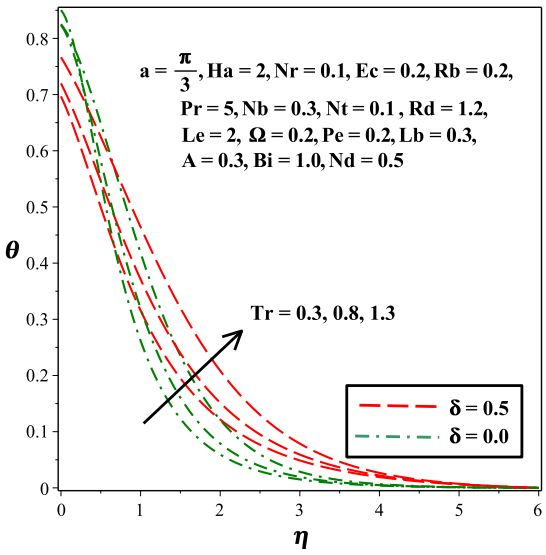

Figure 8: Effect of Tr on temperature field.

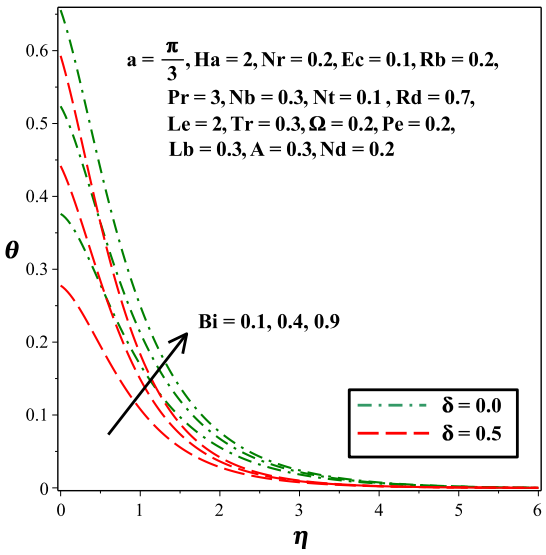

Figure 9: Effect of Bi on temperature field.

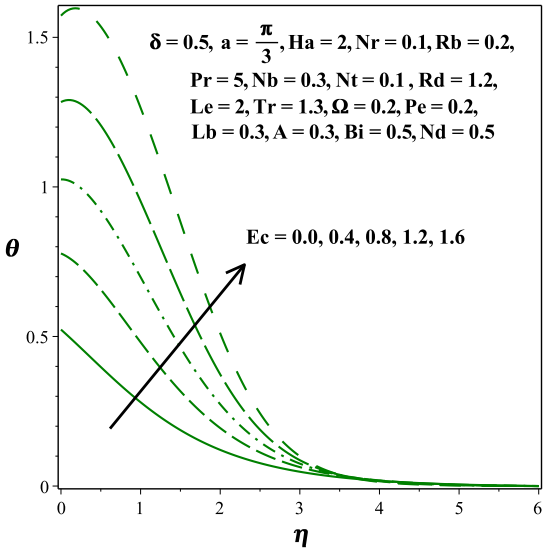

Figure 10: Influence of Eckert number on temperature profile.

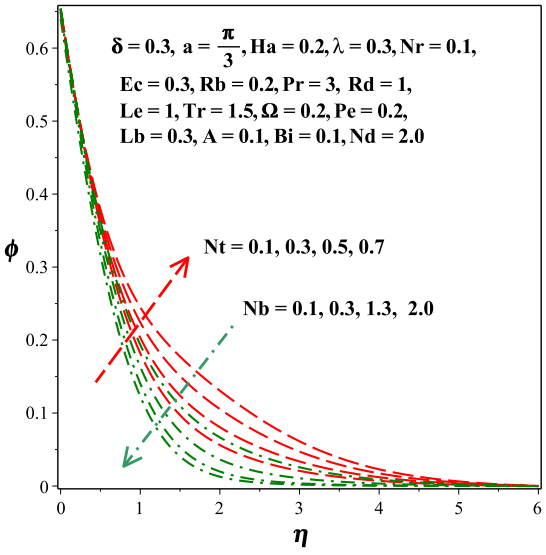

Figure 11: Combine effect of Nt and Nb on concentration profile.

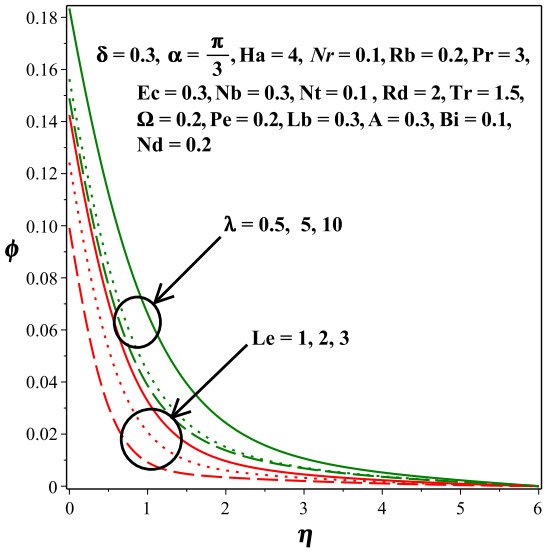

Figure 12: Combine effect of λ and Le on concentration profile.

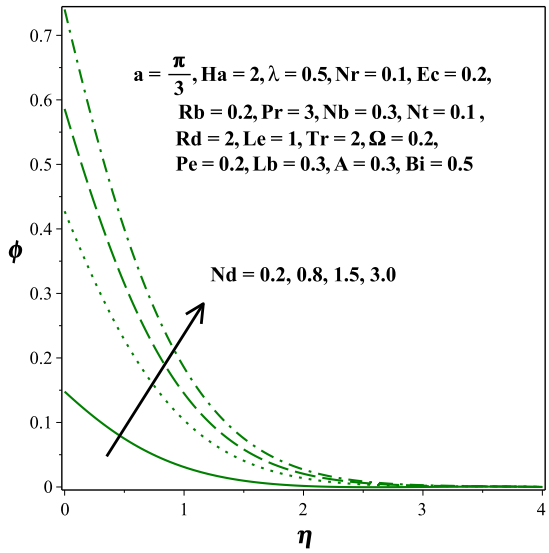

Figure 13: Influence of Nd on concentration distribution.

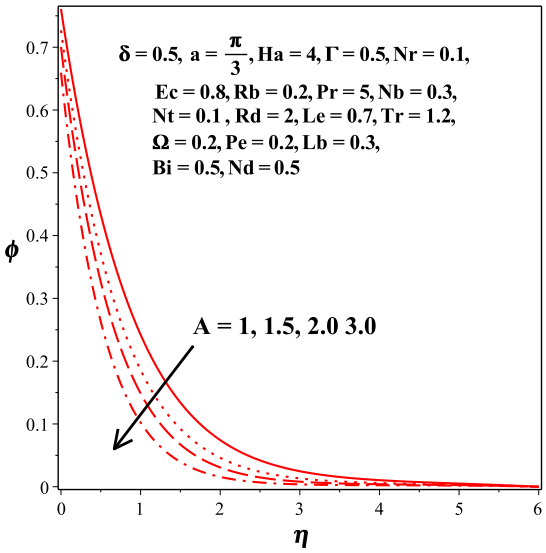

Figure 14: Influence of $A \geq 0$ on concentration distribution.

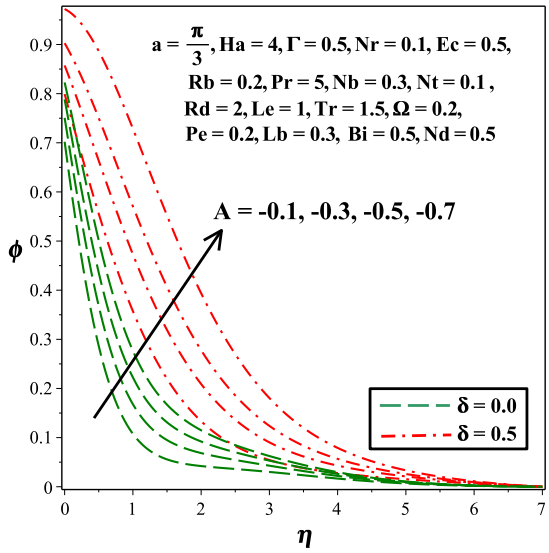

Figure 15: Influence of $A < 0$ on concentration distribution.

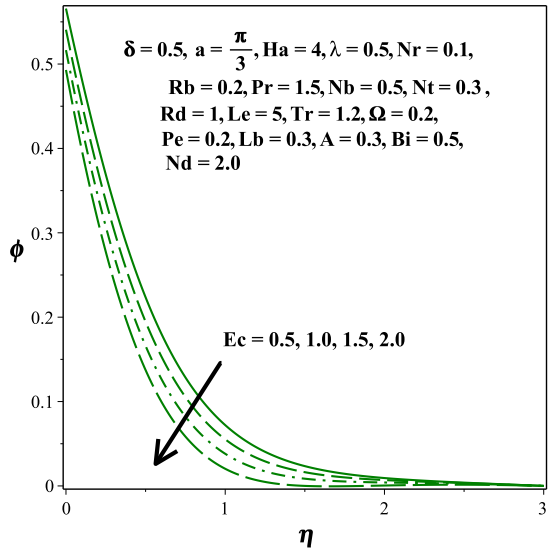

Figure 16: Impact of Eckert number on concentration profile.

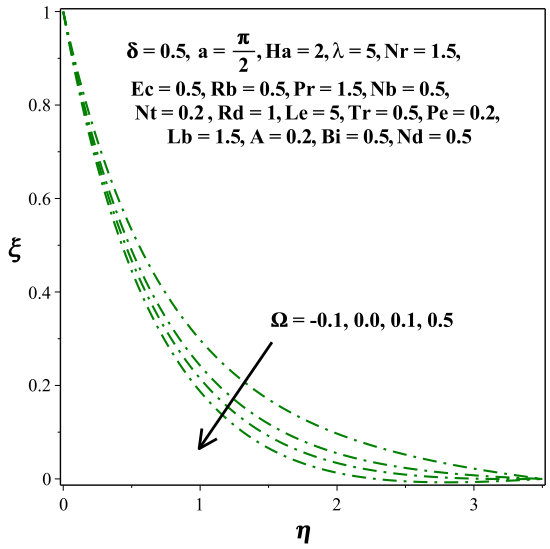

Figure 17: Effect of Ω on density of microorganisms.

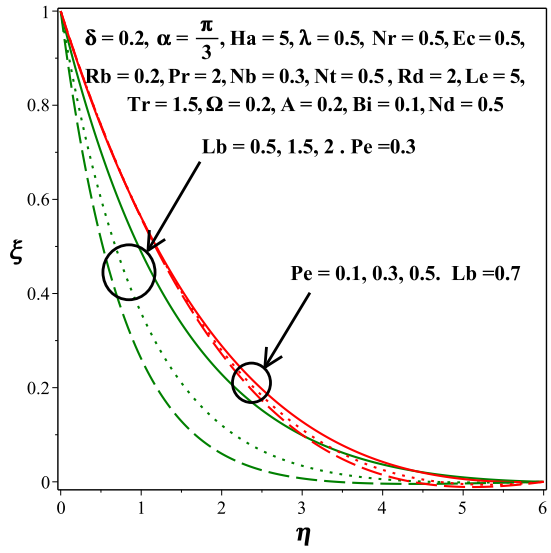

Figure 18: Effects of Lb and Pe on density of microorganisms.

Ha	δ	α	Rb	λ	Nr	$\mathrm{C}_f\ \mathrm{Re}_x^{1/2}$
0.5000	0.2000	$\frac{\pi}{3}$	0.2000	0.1000	0.1000	0.89755
1.0000						0.99027
1.5000						1.07114
2.0000						1.14315
1.0000	0.0000	$\frac{\pi}{3}$	0.2000	0.1000	0.1000	1.30774
	0.4000					0.88870
	0.8000					0.73732
	1.2000					0.63308
1.0000	0.2000	$\frac{\pi}{6}$	0.2000	0.1000	0.1000	0.86318
		$\frac{\pi}{4}$				0.93003
		$\frac{\pi}{3}$				0.99027
		$\frac{\pi}{2}$				1.04528
1.0000	0.2000	$\frac{\pi}{3}$	0.3000	0.1000	0.1000	1.02346
			0.5000			1.05886
			0.7000			1.09480
			1.0000			1.14960
1.0000	0.2000	$\frac{\pi}{3}$	0.2000	0.2000	0.1000	1.01377
				0.4000		1.02570
				0.6000		1.03330
				0.8000		1.03741
1.0000	0.2000	$\frac{\pi}{3}$	0.2000	0.1000	0.3000	1.00692
					0.7000	1.00876
					1.0000	1.01015
					1.5000	1.01246

Table 1: Numerical values of $\mathrm{C}_f\ \mathrm{Re}_x^{1/2}$ when $Nb = 0.5,\ Nt = 0.3,\ Rd = 0.5,\ \mathrm{Pr} = 2,\ Tr = 0.5,\ Ec = 0.1,\ Bi = 0.4,\ Le\ 1.3,\ Nd = 0.2,\ Pe = 1.1,\ Lb = 1.0,\ A = 0.5,\ \Omega = 0.2$.

Rd	Ec	Pr	Nb	Nt	Bi	$\mathrm{Nu}_x\mathrm{Re}_x^{-1/2}$
1.0000	0.2000	3.0000	0.5000	0.3000	0.4000	0.41112
3.0000						0.87397
5.0000						1.33346
7.0000						1.79354
5.0000	0.0000	3.0000	0.5000	0.3000	0.4000	1.44802
	0.1000					1.33346
	0.3000					1.10091
	0.4000					0.98316
5.0000	0.1000	2.0000	0.5000	0.3000	0.4000	1.30966
		4.0000				1.35856
		6.0000				1.41110
		8.0000				1.46448
5.0000	0.1000	3.0000	0.1000	0.3000	0.4000	1.34264
			0.3000			1.33770
			0.5000			1.33345
			0.7000			1.32932
5.0000	0.1000	3.0000	0.5000	0.2000	0.4000	1.34154
				0.4000		1.32539
				0.6000		1.30931
				0.8000		1.29330
5.0000	0.1000	3.0000	0.5000	0.3000	0.5000	1.44507
					1.0000	1.71555
					1.5000	1.82243
					2.0000	1.87950

Table 2: Numerical values of $\mathrm{Nu}_x\mathrm{Re}_x^{-1/2}$ when $\delta = 0.2,\ Ha = 1.0,\ \lambda = 0.1,\ Nd = 0.2,\ Le$ 2.0, $Nr = 0.1,\ Pe = 1.1,\ Tr = 1.5,\ Lb = 1.0,\ Rb = 1.0,\ A = 0.5$.

δ	A	Nd	Le	Nb	Ec	$\mathrm{Sh}_x\mathrm{Re}_x^{-1/2}$
0.2000	0.5000	0.1000	2.0000	0.5000	0.5000	0.09793
0.4000						0.09537
0.6000						0.09375
0.8000						0.09264
0.2000	0.3000	0.1000	2.0000	0.5000	0.5000	0.09665
	0.8000					0.09901
	1.3000					0.09984
	2.0000					0.10024
0.2000	0.5000	0.2000	2.0000	0.5000	0.5000	0.18157
		0.6000				0.42176
		1.0000				0.57353
		1.5000				0.69940
0.2000	0.5000	0.1000	2.0000	0.5000	0.5000	0.09793
			4.0000			0.09805
			6.5000			0.09830
			8.0000			0.09850
0.2000	0.5000	0.1000	2.0000	0.2000	0.2000	0.09047
				0.4000		0.09123
				0.6000		0.09149
				0.8000		0.09162
0.2000	0.5000	0.1000	2.0000	0.5000	0.3000	0.09355
					0.5000	0.09793
					0.7000	0.10233
					0.9000	0.10674

Table 3: Numerical values of $\mathrm{Sh}_x\mathrm{Re}_x^{-1/2}$ when $\lambda = 0.3$, $Rb = Nr = 0.1$, $Ha = 1.0$, $Tr = Rd = 0.5$, $\mathrm{Pr} = 1.2$, $\Omega = 0.2$, $Nt = 0.4$, $Pe = 1.1$, $Lb = 1.0$, $Bi = 0.4$.

δ	Lb	Pe	Ω	Nd	Ec	$\mathrm{Nn}_x\mathrm{Re}_x^{-1/2}$
0.2000	1.0000	0.4000	0.2000	0.1000	0.5000	2.25477
0.4000						2.26452
0.6000						2.27020
0.8000						2.27375
0.2000	1.0000	0.4000	0.2000	0.1000	0.5000	2.17182
	1.5000					2.19356
	2.0000					2.58828
	2.5000					3.04664
0.2000	1.0000	0.0000	0.2000	0.1000	0.5000	1.00248
		0.1000				1.01996
		0.3000				1.34474
		0.4000				2.17182
0.2000	1.0000	0.3000	0.2000	0.1000	0.5000	1.34474
			0.4000			2.14050
			0.6000			2.93722
			0.8000			3.73483
0.2000	1.0000	0.3000	0.2000	0.1000	0.5000	1.34474
				0.3000		1.38330
				0.5000		1.41380
				0.7000		1.43855
0.2000	1.0000	0.3000	0.2000	0.1000	0.2000	1.37588
					0.4000	1.35520
					0.6000	1.33423
					0.8000	1.31324

Table 4: Numerical values of $\mathrm{Nn}_x\mathrm{Re}_x^{-1/2}$ when $\lambda = 0.3$, $Rb = 0.1$, $Ha = 1.0$, $Tr = 0.5$, $Rd = 0.5$, $Nt = 0.4$, $Bi = 0.4$, $\mathrm{Pr} = 2$, $Nb = 0.5$, $Le = 2$, $Nr = 0.1$, $A = 0.4$.

M	$-f''(0)$	
—	[47]	Present
0.0	1.00000	1.0000
0.2	1.01980	1.0198
0.5	1.11803	1.1180
0.8	1.28063	1.2805
1.0	1.41421	1.4141
1.2	1.56205	1.5620
1.5	1.80303	1.8029

Table 5: Comparison of skin-friction coefficient with Shehzad et al. [47] when $\lambda = 0.0,\ \alpha = \pi/2$.

Pr	Bi	Le	$-\theta'(0)$		$-\phi'(0)$	
—	—	—	[48]	Present	[48]	Present
1.0	0.1	5.0	0.0789	0.0789913	1.5477	1.54781
2.0	0.1	5.0	0.0806	0.0806128	1.5554	1.55521
5.0	0.1	5.0	0.0735	0.0734478	1.5983	1.59809
10.0	0.1	5.0	0.0387	0.0386801	1.7293	1.72896
5.0	1.0	5.0	0.1476	0.147565	1.6914	1.69097
5.0	10.0	5.0	0.1550	0.154994	1.7122	1.71176
5.0	100	5.0	0.1557	0.155657	1.7144	1.71391
5.0	∞	5.0	0.1557	0.15573	1.7146	1.71415
5.0	0.1	10.0	0.0647	0.06468	2.3920	2.3918
5.0	0.1	15.0	0.0600	0.0599771	2.9899	2.98983
5.0	0.1	20.0	0.0570	0.0570345	3.4881	3.48798

Table 6: Comparison of Nusselt number and Sherwood number with Makinde and Aziz [48] when $\lambda = 0.0,\ \alpha = \pi/2,\ Rd = 0,\ Nt = Nb = 0.5,\ Tr = 0.0, Nd = \infty$.

5 Concluding remarks

In this article, analysis has been made for the biconveciton nanofluid with gyrotactic microorganism in the presence of non-linear thermal radiation and convective heat and mass boundary conditions. The boundary value problem is analyzed numerically through dsolve method command with numeric option in maple.Following results are deduced from the present analysis.

- Velocity profile exhibits escalating behavior for increasing values of the mixed convection parameter λ.
- Increment in temperature field is observed for increasing values of Biot number radiation and temperature ratio parameter.
- The temperature exhibits rising behavior, while the heat transfer rate diminish for rasing values of viscous dissipation effect.
- The concentration distribution is a decreasing function of Eckert number whereas, the mass transfer rate gives escalating values as the Eckert number increases.
- Concentration profile shows decreasing tendency for increasing values of Lewis number, mixed convection and constructive chemical reaction parameter.
- The motile density of microorganisms indicates decrease in nature for increasing values of bioconvection Lewis number and Peclet number.
- The density number decreases for increasing bioconvection Peclet number.

Acknowledgement:
This work was supported by the World Class 300 Project (No. S2367878) of the SMBA (Korea).

Conflict of Interest:
Authors have no conflict of interest regarding this publication.

References

[1] M. Mustafa, J. A. Khan, T. Hayat, and A. Alsaedi. Buoyancy effects on the mhd nanofluid flow past a vertical surface with chemical reaction and activation energy. *International Journal of Heat and Mass Transfer*, 108:1340–1346, (2017).

[2] M. Ramzan, M. Bilal, J. D. Chung, and A. B. Mann. On mhd radiative jeffery nanofluid flow with convective heat and mass boundary conditions. *Neural Computing and Applications*, pages 1–10.

[3] A. Hussain, M. Y. Malik, T. Salahuddin, S. Bilal, and M. Awais. Combined effects of viscous dissipation and joule heating on mhd sisko nanofluid over a stretching cylinder. *Journal of Molecular Liquids*, 231:341–352, (2017).

[4] A. U. Khan, S. Nadeem, and S. T. Hussain. Phase flow study of mhd nanofluid with slip effects on oscillatory oblique stagnation point flow in view of inclined magnetic field. *Journal of Molecular Liquids*, 224:1210–1219, (2016).

[5] S. U. S. Choi. Enhancing thermal conductivity of fluids with nanoparticles. *ASME-Publications-Fed*, 231:99–106, (1995).

[6] M. Sheikholeslami and D. D. Ganji. Numerical approach for magnetic nanofluid flow in a porous cavity using cuo nanoparticles. *Materials & Design*, 120:382–393, (2017).

[7] M. M. Rashidi, A. K. Abdul Hakeem, N. Vishnu Ganesh, B. Ganga, M. Sheikholeslami, and E. Momoniat. Analytical and numerical studies on heat transfer of a nanofluid over a stretching/shrinking sheet with second-order slip flow model. *International Journal of Mechanical and Materials Engineering*, 11(1):1–14, (2016).

[8] R. Mehmood, S. Nadeem, S. Saleem, and N. S. Akbar. Flow and heat transfer analysis of jeffery nano fluid impinging obliquely over a stretched plate. *Journal of the Taiwan Institute of Chemical Engineers*, (2017).

[9] T. Hayat, T. Muhammad, S. A. Shehzad, and A. Alsaedi. An analytical solution for magnetohydrodynamic Oldroyd-b nanofluid flow induced by a stretching sheet with heat generation/absorption. *International Journal of Thermal Sciences*, 111:274–288, (2017).

[10] M. Ramzan and M. Bilal. Time dependent MHD nano-second grade fluid flow induced by permeable vertical sheet with mixed convection and thermal radiation. *PloS one*, 10(5):e0124929, (2015).

[11] M. Ramzan and M. Bilal. Three-dimensional flow of an elastico-viscous nanofluid with chemical reaction and magnetic field effects. *Journal of Molecular Liquids*, 215:212–220, (2016).

[12] T. Hussain, S. A. Shehzad, T. Hayat, A. Alsaedi, F. Al-Solamy, and M. Ramzan. Radiative hydromagnetic flow of Jeffrey nanofluid by an exponentially stretching sheet. *Plos One*, 9(8):e103719, (2014).

[13] M. Ramzan and F. Yousaf. Boundary layer flow of three-dimensional viscoelastic nanofluid past a bi-directional stretching sheet with Newtonian heating. *AIP Advances*, 5(5):057132, (2015).

[14] M. Ramzan. Influence of Newtonian heating on three dimensional MHD flow of couple stress nanofluid with viscous dissipation and joule heating. *PloS one*, 10(4):e0124699, (2015).

[15] T. Hussain, S. A. Shehzad, A. Alsaedi, T. Hayat, and M. Ramzan. Flow of Casson nanofluid with viscous dissipation and convective conditions: a mathematical model. *Journal of Central South University*, 22(3):1132–1140, (2015).

[16] M. Ramzan, M. Bilal, J. D. Chung, and U. Farooq. Mixed convective flow of Maxwell nanofluid past a porous vertical stretched surface–An optimal solution. *Results in Physics*, 6:1072–1079, (2016).

[17] M. Ramzan, M. Bilal, U. Farooq, and J. D. Chung. Mixed convective radiative flow of second grade nanofluid with convective boundary conditions: An optimal solution. *Results in Physics*, 6:796–804, (2016).

[18] T. J. Pedley and J. O. Kessler. Hydrodynamic phenomena in suspensions of swimming microorganisms. *Annual Review of Fluid Mechanics*, 24(1):313–358, (1992).

[19] H. Wager. The effect of gravity upon the movements and aggregation of euglena viridis, ehrb., and other micro-organisms. *Proceedings of the Royal Society of London. Series B, Containing Papers of a Biological Character*, 83(562):94–96, (1910).

[20] J. O. Kessler. Hydrodynamic focusing of motile algal cells. (1985).

[21] D. F. Katz and L. Pedrotti. Geotaxis by motile spermatozoa hydrodynamic reorientation. *Journal of theoretical biology*, 67(4):723–732, (1977).

[22] T. Fenchel and B. J. Finlay. Geotaxis in the ciliated protozoon loxodes. *Journal of experimental Biology*, 110(1):17–33, (1984).

[23] R. V. Vincent and N. A. Hill. Bioconvection in a suspension of phototactic algae. *Journal of Fluid Mechanics*, 327:343–371, (1996).

[24] M. J. Schnitzer, S. M. Block, and H. C. Berg. Strategies for chemotaxis. *Biology of the chemotactic response*, 46:15, (1990).

[25] J. Shioi, C. V. Dang, and B. L. Taylor. Oxygen as attractant and repellent in bacterial chemotaxis. *Journal of bacteriology*, 169(7):3118–3123, (1987).

[26] T. J. Pedley and J. O. Kessler. A new continuum model for suspensions of gyrotactic micro-organisms. *Journal of Fluid Mechanics*, 212:155–182, (1990).

[27] A. V. Kuznetsov. Non-oscillatory and oscillatory nanofluid bio-thermal convection in a horizontal layer of finite depth. *European Journal of Mechanics-B/Fluids*, 30(2):156–165, (2011).

[28] A. V. Kuznetsov. Nanofluid bioconvection in porous media: Oxytactic microorganisms. *Journal of Porous Media*, 15(3), (2012).

[29] T. H. Tsai, D. S. Liou, L. S. Kuo, and P. H. Chen. Rapid mixing between ferro-nanofluid and water in a semi-active y-type micromixer. *Sensors and Actuators A: Physical*, 153(2):267–273, (2009).

[30] A. V. Kuznetsov. The onset of thermo-bioconvection in a shallow fluid saturated porous layer heated from below in a suspension of oxytactic microorganisms. *European Journal of Mechanics-B/Fluids*, 25(2):223–233, (2006).

[31] N. S. Akbar and Z. H. Khan. Magnetic field analysis in a suspension of gyrotactic microorganisms and nanoparticles over a stretching surface. *Journal of Magnetism and Magnetic Materials*, 410:72–80, (2016).

[32] L. Tham, R. Nazar, and I. Pop. Mixed convection flow over a solid sphere embedded in a porous medium filled by a nanofluid containing gyrotactic microorganisms. *International Journal of Heat and Mass Transfer*, 62:647–660, (2013).

[33] A. Aziz, W. A. Khan, and I. Pop. Free convection boundary layer flow past a horizontal flat plate embedded in porous medium filled by nanofluid containing gyrotactic microorganisms. *International Journal of Thermal Sciences*, 56:48–57, (2012).

[34] W. A. Khan and O. D. Makinde. Mhd nanofluid bioconvection due to gyrotactic microorganisms over a convectively heat stretching sheet. *International Journal of Thermal Sciences*, 81:118–124, (2014).

[35] W. N. Mutuku and O. D. Makinde. Hydromagnetic bioconvection of nanofluid over a permeable vertical plate due to gyrotactic microorganisms. *Computers & Fluids*, 95:88–97, (2014).

[36] S. A. M. Mehryan, F. M. Kashkooli, M. Soltani, and K. Raahemifar. Fluid flow and heat transfer analysis of a nanofluid containing motile gyrotactic micro-organisms passing a nonlinear stretching vertical sheet in the presence of a non-uniform magnetic field; numerical approach. *PloS one*, 11(6):e0157598, (2016).

[37] H. Xu and I. Pop. Fully developed mixed convection flow in a horizontal channel filled by a nanofluid containing both nanoparticles and gyrotactic microorganisms. *European Journal of Mechanics-B/Fluids*, 46:37–45, (2014).

[38] S. Siddiqa, M. Sulaiman, M. A. Hossain, S. Islam, and R. S. R. Gorla. Gyrotactic bioconvection flow of a nanofluid past a vertical wavy surface. *International Journal of Thermal Sciences*, 108:244–250, (2016).

[39] O. D. Makinde and I. L. Animasaun. Bioconvection in mhd nanofluid flow with nonlinear thermal radiation and quartic autocatalysis chemical reaction past an upper surface of a paraboloid of revolution. *International Journal of Thermal Sciences*, 109:159–171, (2016).

[40] A. Raees, M. Raees-ul Haq, H. Xu, and Q. Sun. Three-dimensional stagnation flow of a nanofluid containing both nanoparticles and microorganisms on a moving surface with anisotropic slip. *Applied Mathematical Modelling*, 40(5):4136–4150, (2016).

[41] C. S. K. Raju and N. Sandeep. Heat and mass transfer in mhd non-newtonian bio-convection flow over a rotating cone/plate with cross diffusion. *Journal of Molecular Liquids*, 215:115–126, (2016).

[42] M. S. Hoecker-Martínez and W. D. Smyth. Trapping of gyrotactic organisms in an unstable shear layer. *Continental Shelf Research*, 36:8–18, (2012).

[43] N. Acharya, K. Das, and P. K. Kundu. Framing the effects of solar radiation on magneto-hydrodynamics bioconvection nanofluid flow in presence of gyrotactic microorganisms. *Journal of Molecular Liquids*, 222:28–37, (2016).

[44] A. Alsaedi, M. I. Khan, M. Farooq, N. Gull, and T. Hayat. Magnetohydrodynamic (mhd) stratified bioconvective flow of nanofluid due to gyrotactic microorganisms. *Advanced Powder Technology*, (2016).

[45] Maplesoft. http://de.maplesoft.com/support/help/Maple/view.aspx?path=dsolve

[46] S. Rosseland. *Astrophysik: Auf Atomtheoretischer Grundlage*, volume 11. Springer-Verlag, (2013).

[47] S. A. Shehzad, T. Hayat, and A. Alsaedi. Influence of convective heat and mass conditions in mhd flow of nanofluid. *Bulletin of the Polish Academy of Sciences Technical Sciences*, 63(2):465–474, (2015).

[48] O. D. Makinde and A. Aziz. Boundary layer flow of a nanofluid past a stretching sheet with a convective boundary condition. *International Journal of Thermal Sciences*, 50(7):1326–1332, (2011).